Responsive Particle Dynamics for Modeling Solvents on the Mesoscopic Scale

Wim Briels

Computational Biophysics, University of Twente
P.O. Box 217, 7500AE Enschede, The Netherlands
and
Forschungszentrum Jülich, ICS 3, D-52425 Jülich, Germany

E-mail: w.j.briels@utwente.nl

In this chapter we will review the standard ways to perform stochastic simulations on soft matter without memory. In order to make these methods available for very concentrated complex polymeric soft matter in which the particles experience large frictions we will extend these models to include memory and hydrodynamics at the Brownian level. This allows us to study flow instabilities and even flow in complex geometries.

1 Introduction

It is our intention in this paper to describe a model for simulating complex soft matter systems, possibly flowing through complex geometries, and possibly undergoing phase transitions or flow instabilities. This requires that the model faithfully represents all thermodynamic and all rheological properties of the system. The simplest way to do this would be to perform a full glory particle based simulation, if not this would be impossible because of prohibitively large computational costs (just to make an understatement). Yet this is more or less what we want to do, although we will have to remove the adjective 'full glory'.

Complex soft matter systems usually consist of very large particles with many internal degrees of freedom, dissolved in an appropriate solvent or in the molten state. The prototypical example of a particle is a star polymer of hundreds of kilo-Daltons. We will develop a severely coarse-grained simulation model for such a system, in which each molecule is represented by just its center of mass position. This requires special tricks of course, as can be understood from a glance at Fig. (1). In the left panel of this figure we have depicted an artist's impression of a star polymer solution. Each polymer consists of many arms connected to a central point. The concentration is such that the arms of each polymer are highly entangled with many of their neighbors. One of the characteristics of polymers as opposed to normal molecules is that they interact with hundreds of neighbors, not just something between ten and twenty as in dense liquids or solutions of normal molecules. Now, the act/art of coarse-graining is to remove all explicit reference to the internal degrees of freedom of each molecule and the degrees of freedom of the solvent. Once we have done this, our system looks geometrically like the right hand panel of Fig. (1). This looks very much like an ideal gas, yet we have to make the particles move like the centers of mass do in the the left hand panel.

We will gradually build the theory underlying the model that we need. We start by reviewing the theory behind the Langevin equation that describes the motion of colloidal

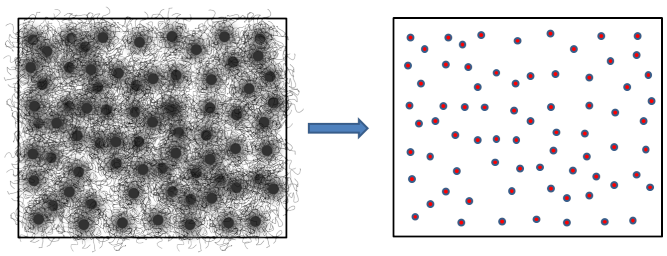

Figure 1: Definition of coarse-graining. In the left panel a complex soft matter system is depicted, consisting of star polymers dissolved in a solvent. Each star consists of many arms connected to a central point, while each arm is a polymer of many kilo Daltons of mass. The concentration is such that each star interacts with many, usually hundreds, of neighboring fellows. In the right panel we have depicted what the system looks like when only centers of mass are seen. This is what is simulated by our coarse model. The dynamics of the points in the right panel must be equal to that of the centers of mass in the left panel.

particles in a solvent. Next we discuss changes to be made in order to make the model applicable to our aimed for systems. In section 4 we notice that momenta usually play no role in soft matter systems and that it is better to dispense with them altogether. The result of this section will be the final model that we apply in our simulations. It describes displacements of the particles with respect to a background flow which drags them along. Our algorithm includes updates to calculate the time evolution of the background flow. Interactions between particles will be such that they give rise to correct thermodynamical behavior of the system. A reasonably small set of structural variables is introduced to describe memory effects that result from the fact that every configuration of the coarse degrees of freedom on the small scale may be accompanied by one of many configurations of the eliminated degrees of freedom. These variables describe how the eliminated dgrees of freedom would have responded to the changing coarse configurations. The method therefore carries the name of Resposive Particle Dynamics (RaPiD). It is important that the additional structural variables do not influence the thermodynamics of the system. Finally in section 5 we describe one example that has been simulated using this method.

2 The Langevin Equation

Our discussion in this section will be very much along the lines of McQuarrie's textbook on Statistical Physics[1]. The prototypical example of a system to which stochastic differential equations are applied is the infinitely diluted suspension of colloids in an appropriate solvent. In this case each colloidal particle can be assumed to move independently of all other particles, while only being influenced by the surrounding solvent molecules. In the usual explanation of the action of the solvent molecules on the colloid it is assumed, that while the colloid moves through the liquid, it experiences more collisions with the solvent molecules in the front than in its back. This gives rise, on average, to a force opposite to the direction of its motion and proportional to the absolute value of its velocity. The deviation of the instantaneous force from this average force is then a quickly fluctuating contribution, which on average equals zero. The corresponding equation of motion for the

colloid is called the Langevin equation and reads

$$m\frac{d\mathbf{v}}{dt} = -\xi\mathbf{v} + \mathbf{F}^{ran}. \tag{1}$$

Here $\mathbf{v}$ denotes the velocity of the particle and m its mass; ξ is called the friction coefficient and $\mathbf{F}^{ran}$ the random force. Notice that the dimensions of ξ are kg/s. Below we will prove that the random forces are related to the friction coefficient according to

$$< \mathbf{F}^{ran}(t)\mathbf{F}^{ran}(0) >= 2\xi k_B T\delta(t)\mathbf{1}. \tag{2}$$

The latter equation is called the Fluctuation-Dissipation theorem.

The left hand side of Eq. (2) should be read like

$$\begin{pmatrix} < F_x^{ran}(t)F_x^{ran}(0) > & < F_x^{ran}(t)F_y^{ran}(0) > & < F_x^{ran}(t)F_z^{ran}(0) > \\ < F_y^{ran}(t)F_x^{ran}(0) > & < F_y^{ran}(t)F_y^{ran}(0) > & < F_y^{ran}(t)F_z^{ran}(0) > \\ < F_z^{ran}(t)F_x^{ran}(0) > & < F_z^{ran}(t)F_y^{ran}(0) > & < F_z^{ran}(t)F_z^{ran}(0) > \end{pmatrix} \tag{3}$$

Pointy brackets in general indicate an equilibrium average. When we average the product of two variables taken at different times, the interpretation is a bit more involved. In the present case, $< F_\alpha^{ran}(t)F_\beta^{ran}(0) >$ is called the time correlation function of the random forces in α and β direction. It is the average value of $F_\alpha^{ran}(t)$ at time t over all realizations which had $F_\beta^{ran}(0)$ at time $t = 0$, multiplied by $F_\beta^{ran}(0)$ and next averaged over all possible realizations. A realization is just a time sequence of positions of the colloidal particle under investigation. A practical way to calculate $< F_\alpha^{ran}(t)F_\beta^{ran}(0) >$ from a realization of length T is

$$< F_\alpha^{ran}(t)F_\beta^{ran}(0) >= \frac{1}{T-t}\int_0^{T-t} d\tau F_\alpha^{ran}(\tau+t)F_\beta^{ran}(\tau) \tag{4}$$

$\mathbf{1}$ is the 3×3 unit matrix. Moreover, $\delta(t)$ is the Dirac delta, which may be thought of as an infinitely narrow function centered at $t = 0$ and whose integral is equal to unity. For its numerical treatment see the section on Brownian Dynamics.

Next consider a dense system of N colloids which interact via a potential $\Phi(r^{3N})$, where $r^{3N} = \{\mathbf{r}_1, \mathbf{r}_2, ..., \mathbf{r}_N\}$. A conservative force

$$\mathbf{F}_i = -\nabla_i\Phi \tag{5}$$

then acts on particle i. We assume that the Langevin equation for particle i may be obtained by adding a subscript i to all quantities and by adding $-\nabla_i\Phi$ in the right hand side of Eq. (1). Besides this we assume that the frictions and random forces are not influenced by these extensions. The final equations then read:

$$m_i\frac{d\mathbf{v}_i}{dt} = -\nabla_i\Phi - \xi_i\mathbf{v}_i + \mathbf{F}_i^{ran}, \tag{6}$$

$$< \mathbf{F}_i^{ran}(t)\mathbf{F}_j^{ran}(0) >= 2\xi_i k_B T\delta(t)\delta_{ij}\mathbf{1}. \tag{7}$$

Here we have assumed that random forces acting on different particles are uncorrelated, which is reflected in the Kronecker delta δ_{ij} in the right hand side of the Fluctuation-Dissipation theorem, which equals unity when $i = j$ and zero otherwise.

Let me finally notice that we have ignored the possibility that moving one particle has an influence on other particles via the flow field induced in the solvent. The corresponding

interactions are called hydrodynamic interactions. They are indeed relevant for colloidal suspensions in Newtonian fluids, but play a minor role in the applications of stochastic methods presented in his chapter.

2.1 Fluctuation Dissipation theorem

In this section we restrict ourselves again to particles moving independently from each other in absence of any external fields. It will be assumed that friction forces and corresponding random forces, resulting from interactions with the solvent, are independent of possible interactions between the particles. Only in the case of hydrodynamic interactions a more general treatment is needed.

In order to prove the Fluctuation-Dissipation theorem we notice that

$$\mathbf{v}(t) = \mathbf{v}(0)e^{-\xi t/m} + \frac{1}{m}\int_0^t dt' e^{-\xi(t-t')/m}\mathbf{F}^{ran}(t') \tag{8}$$

solves the Langevin equation for the initial velocity $\mathbf{v}(0)$. We next invoke the equipartition theorem of statistical physics, which says that, in equilibrium, velocities along different Cartesian axes are uncorrelated, *i.e.* that $< v_\alpha(t)v_\beta(t) >=< v_\alpha(t) >< v_\beta(t) >= 0$ in case $\alpha \neq \beta$, while $< v_\alpha(t)v_\alpha(t) >= k_BT/m$. In order to make the particle forget its initial velocity and to reach equilibrium, we must take the limit of $t \longrightarrow \infty$ in the above solution. The equipartition theorem then says

$$\lim_{t\to\infty} < \mathbf{v}(t)\mathbf{v}(t) >= \frac{k_BT}{m}\mathbf{1}. \tag{9}$$

Inserting Eq. (8) we obtain

$$\lim_{t\to\infty} \frac{1}{m^2}\int_0^t dt' \int_0^t dt'' e^{-\xi(2t-t'-t'')/m} < \mathbf{F}^{ran}(t')\mathbf{F}^{ran}(t'') >= \frac{k_BT}{m}\mathbf{1}. \tag{10}$$

Next we make use of $< \mathbf{F}^{ran}(t')\mathbf{F}^{ran}(t'') >=< \mathbf{F}^{ran}(t''-t')\mathbf{F}^{ran}(0) >$ and change integration variables to $\tau' = t'' + t'$ and $\tau'' = t'' - t$, obtaining

$$\lim_{t\to\infty} \frac{1}{2m^2}\int_0^{2t} d\tau' \int_{-t}^{t} d\tau'' e^{-\xi(2t-\tau')/m} < \mathbf{F}^{ran}(\tau'')\mathbf{F}^{ran}(0) >= \frac{k_BT}{m}\mathbf{1}. \tag{11}$$

Performing the integral over τ' we obtain

$$\int_{-t}^{t} d\tau'' < \mathbf{F}^{ran}(\tau'')\mathbf{F}^{ran}(0) >= 2\xi k_BT\mathbf{1}. \tag{12}$$

If we next assume that the time-correlation functions of the random forces are very short lived, expressed as $< F_i^{ran}(t)F_i^{ran}(0) >= C\delta(t)$, and perform the final integral, we obtain the Fluctuation-Dissipation theorem.

2.2 Einstein equation

We now integrate the equations of motion once more in order to obtain displacements. Also in this subsection we ignore effects of interactions and external fields on the displacements of the particles and concentrate on the contributions from the solvent.

Integrating Eq. (8) we obtain

$$\mathbf{r}(t) - \mathbf{r}(0) = \mathbf{v}(0)\frac{m}{\xi}(1 - e^{-\xi t/m}) + \frac{1}{m}\int_0^t dt' \int_0^{t'} dt'' e^{-\xi(t'-t'')/m}\mathbf{F}^{ran}(t''). \quad (13)$$

By interchanging integrations we simplify the second term in the right hand side, obtaining

$$\frac{1}{m}\int_0^t dt'' \int_{t''}^t dt' e^{-\xi(t'-t'')/m}\mathbf{F}^{ran}(t'') = \frac{1}{\xi}\int_0^t dt''(1 - e^{-\xi(t-t'')/m})\mathbf{F}^{ran}(t''). \quad (14)$$

Using the Fluctuation-Dissipation theorem it is now a simple task to calculate

$$\begin{aligned} < \Delta\mathbf{r}(t)\Delta\mathbf{r}(t) > = & \frac{m^2}{\xi^2}(1 - e^{-\xi t/m})^2\mathbf{v}(0)\mathbf{v}(0) \\ & + \frac{k_B T}{\xi}(2t - 3\frac{m}{\xi} + 4\frac{m}{\xi}e^{-\xi t/m} - \frac{m}{\xi}e^{-2\xi t/m})\mathbf{1}, \end{aligned} \quad (15)$$

where $\Delta\mathbf{r}(t) = \mathbf{r}(t) - \mathbf{r}(0)$. Usually we are interested in equilibrium situations, where we may average the first term over the Maxwell distribution, obtaining $< \mathbf{v}(0)\mathbf{v}(0) >= \frac{k_B T}{m}\mathbf{1}$ and

$$< \Delta\mathbf{r}(t)\Delta\mathbf{r}(t) >= 2\frac{k_B T}{\xi}(t - \frac{m}{\xi} + \frac{m}{\xi}e^{-\xi t/m})\mathbf{1}. \quad (16)$$

For times t much larger than $\frac{m}{\xi}$ we may neglect the last two terms. We then calculate the mean square displacement by taking the trace

$$< \Delta\mathbf{r}(t) \cdot \Delta\mathbf{r}(t) >= Tr < \Delta\mathbf{r}(t)\Delta\mathbf{r}(t) >= 6Dt, \quad (17)$$

where

$$D = \frac{k_B T}{\xi}. \quad (18)$$

D is called diffusion coefficient and Eq. (18) the Einstein relation.

3 Application to Complex Soft Matter

In this section we will address the various terms in the Langevin equation from the perspective of its application to complex, visco-elastic soft matter systems. The prototypical system to have in mind is that of a melt or concentrated solution of highly branched polymers. Our intention is to reduce the degrees of freedom of each polymer to include only its three positional degrees of freedom. This means that all solvent molecules and all internal degrees of freedom of the polymers are eliminated from our description and can only influence the dynamics of the polymers via the three terms in the right hand side of the Langevin equation. For more information, see Briels[2] and van den Noort *et. al.*[3].

3.1 Potential of mean force

The main difference between simple molecular fluids and polymer systems is that simple molecules are rather compact objects packed in a liquid such that they interact with about ten to twenty neighboring fellow molecules, while polymers are large open structures interacting with hundreds of other polymers. As a result the usual assumption of pair wise additive interactions will not be applicable to the case of highly coarse-grained polymer solutions or melts.

In order to get a better understanding of the interactions in polymer systems, notice that $-\nabla_i \Phi$ is the average force on coarse particle i in case all velocities are equal to zero, *i.e.* for a fixed configuration $r^{3N} = \{\mathbf{r}_1, \mathbf{r}_2, ..., \mathbf{r}_N\}$. Denoting the potential energy of the fully detailed microscopic system as $V(r^{3N}, q^M)$, where q^M denotes all the eliminated degrees of freedom, the average force on particle i reads

$$\mathbf{F}_i = -\frac{\int dq^M \nabla_i V(r^{3N}, q^M) \exp\{-\beta V(r^{3N}, q^M)\}}{\int dq^M \exp\{-\beta V(r^{3N}, q^M)\}}. \tag{19}$$

Here we have assumed that dq^M includes possible Jacobians necessary to provide the correct volume element. Comparison of this expression and $\mathbf{F}_i = -\nabla_i \Phi$ leads to

$$\Phi(r^{3N}) = -k_B T \ln \int dq^M \exp\{-\beta V(r^{3N}, q^M)\}. \tag{20}$$

This says that $\Phi(r^{3N})$ is the free energy of the eliminated degrees of freedom, *i.e.* the q^M, in the presence of the field provided by the retained coordinates r^{3N}. Now with Φ being a free energy we write

$$\Phi(r^{3N}) = \sum_{i=1}^{N} a(\eta_i(r^{3N})), \tag{21}$$

where $a(\eta_i(r^{3N}))$ is the free energy per polymer in a system with polymer volume fraction equal to the local volume fraction $\eta_i(r^{3N})$, with the contribution of the center of mass excluded. The local volume fraction may be defined as

$$\eta_i(r^{3N}) = \frac{1}{\rho_{max}} \sum_{j=1}^{N} w(r_{ij}), \tag{22}$$

where ρ_{max} is the maximum polymer (number) density and $w(r)$ some normalized, monotonously decaying weight function with a range on the order of two or three times the radius of gyration of the polymers; the normalization is such that $\int d^3 r w(r) = 1$.

A popular expression for the free energy per polymer (excluding the contribution of its center of mass) derives from the Flory-Huggins free energy[4].

3.2 Memory

One of the characteristics of complex polymer solutions or melts is their visco-elasticity. In order to include the effects of visco-elasticity, the Langevin equation may be generalized to read

$$m_i \frac{d\mathbf{v}_i}{dt} = -\nabla_i \Phi - \int_0^t dt' \mathbf{v}_i(t') \cdot \boldsymbol{\zeta}_i(t - t'; r^{3N}(t')) + \mathbf{F}_i^{ran}, \tag{23}$$

$$< \mathbf{F}_i^{ran}(t)\mathbf{F}_j^{ran}(0) >= k_B T \boldsymbol{\zeta}_i(t; r^{3N}(0))\delta_{ij}. \tag{24}$$

Here $\boldsymbol{\zeta}_i$ is a 3×3 matrix which is multiplied into the vector $\mathbf{v}_i$. Besides this, we have assumed that the total friction force on particle i depends on its velocity at all times t' prior to t and that the corresponding friction tensor $\boldsymbol{\zeta}_i$ depends on the configuration r^{3N} time t'. The generalized friction is said to include 'memory'. We will not prove the Fluctuation-Dissipation theorem as given in Eq. (24). Notice however, that if we assume $\boldsymbol{\zeta}_i(t; r^{3N}(0)) = 2\xi_i\delta(t)\mathbf{1}$ we get back Eqs (6) and (7). Note also that, again, we neglect hydrodynamic interactions.

Let us now try to understand Eq. (23). Within the present context it is useful to rewrite the memory term to read

$$-\int_0^t d\mathbf{r}_i(t') \cdot \boldsymbol{\zeta}_i(t - t'; r^{3N}(t')). \tag{25}$$

This equation reveals the possibility of an entirely different interpretation of the friction term than the one used at the beginning of this chapter to motivate the original Langevin equation Eq. (1). It says that if we displace a particle by $d\mathbf{r}_i(t')$, at all times t after t' the particle will experience a force opposing the displacement and being linear in its components. The strength of the force will gradually fade away with increasing time lapse $t - t'$ after the displacement. The total force at time t is simply the sum of all contributions from displacements in the past.

From a computational point of view Eqs (23) and (24) constitute a very complicated set of equations. Not only do we need to keep track of a usually long history of configurations in order to calculate the friction tensor, but also do we have to sample random forces from complicated coupled distributions to guarantee that the Fluctuation-Dissipation condition Eq. (24) is met. We would rather prefer to deal with the so called Markovian situation where the friction depends only on the instantaneous configuration. Let us therefore investigate a bit closer the meaning of the friction term.

To simplify our considerations we concentrate on one particular displacement $d\mathbf{r}_i(t')$. As a result of this displacement the environment of the particle, in a more detailed treatment described by the eliminated degrees of freedom q^M, will be slightly perturbed to a non-equilibrium configuration. This leads to a force that is slightly different from the average force $-\nabla_i\Phi$ that goes with the new configuration. The difference is what is described by $-d\mathbf{r}_i(t') \cdot \boldsymbol{\zeta}_i(t - t'; r^{3N}(t'))$. With increasing time t it gradually fades away because the eliminated degrees of freedom relax to their new equilibrium state. So, friction in a visco-elastic material basically results from non-equilibrium of the eliminated coordinates.

The above strongly suggests that we restore the slowly evolving part of the friction force, *i.e.* its memory part, back into the conservative force that derives from the free energy Φ. The fast evolving part of the friction force may then be included as a Markovian friction force. To this end we introduce structural parameters $\lambda^m = \{\lambda_1, \lambda_2, ..., \lambda_m\}$, which together describe the thermodynamic state of the eliminated degrees of freedom. At equilibrium they take values $\lambda_{eq}^m(r^{3N}) = \{\lambda_1^{eq}(r^{3N}), \lambda_2^{eq}(r^{3N}), ..., \lambda_m^{eq}(r^{3N})\}$. We next assume that the conservative potential Φ may be replaced by $A(r^{3N}, \lambda^m) = \Phi(r^{3N}) + \Phi^t(r^{3N}, \lambda^m)$ with

$$\Phi^t(r^{3N}, \lambda^m) = \frac{1}{2}\sum_{s=1}^{m} \alpha_s(\lambda_s - \lambda_s^{eq}(r^{3N}))^2. \tag{26}$$

We assume that the λ_s have no dimensions, which implies that the α_s have dimensions of energy. Φ^t is called the transient potential, and the corresponding forces $-\nabla_i \Phi^t$ are called transient forces. For brevity of notation we define

$$A(r^{3N}, \lambda^m) = \Phi(r^{3N}) + \Phi(r^{3N}, \lambda^m) \tag{27}$$

and call it (total) free energy.

3.3 Flow

An obvious short-coming of the Langevin equation presented so far is the fact that the possibility of a moving background is not accounted for. Obviously the friction felt by a particle results not from its absolute motion, but from its velocity with respect to the velocity of the background, *i.e.* the average local velocity of the eliminated degrees of freedom. This can easily be incorporated into the Langevin equation by replacing $-\xi_i \mathbf{v}_i$ by $-\xi_i[\mathbf{v}_i - \mathbf{V}(\mathbf{r}_i)]$, so

$$m_i \frac{d\mathbf{v}_i}{dt} = -\nabla_i A - \xi_i[\mathbf{v}_i - \mathbf{V}(\mathbf{r}_i)] + \mathbf{F}_i^{ran}. \tag{28}$$

This addition makes it necessary to have a model to estimate the local background velocity $\mathbf{V}(\mathbf{r}_i)$ at the position of the particle $\mathbf{r}_i$. We will present a possible way to do this in the section on Brownian Dynamics.

It is appropriate at this point to mention a different way to deal with flowing systems. This is done in Dissipative Particle Dynamics (DPD) by introducing pairwise frictions, which automatically conserve momenta and give rise to a Galilei invariant algorithm[5]. We will not discuss this method here, as it cannot be easily adapted to the case of overdamped systems, *i.e.* systems with very large friction forces.

4 Brownian Dynamics

In many applications of stochastic simulations to soft matter the friction coefficient ξ_i is very large, which we call the overdamped case. In these cases the time step becomes limited, not by the rapidity with which the conservative forces change, but by the contributions of the random forces which become very large.

This can be seen from a naive integration of the Langevin equation:

$$m_i d\mathbf{v}_i = -\nabla_i A dt - \mathbf{v}_i \xi_i dt + \sqrt{\frac{2k_B T \xi_i}{dt}} \mathbf{\Theta}_i dt. \tag{29}$$

Here $\mathbf{\Theta}_i$ is a random vector characterised by $< \Theta_{i,\alpha} >= 0$ and

$$< \Theta_{i,\alpha} \Theta_{i,\beta} >= \delta_{\alpha\beta}. \tag{30}$$

Notice that with the last term in Eq. (29) we have represented the random force $\mathbf{F}_i^{ran}$ by $\sqrt{2k_B T \xi_i / dt}\mathbf{\Theta}_i$. Obviously this equals zero on average, while

$$< F_{i,\alpha}^{ran} F_{i,\beta}^{ran} >= \frac{2k_B T \xi_i}{dt} \delta_{\alpha\beta}. \tag{31}$$

Indeed, when dealing with discretized time, $\delta(t) = 1/dt$, so the last equation agrees with the Fluctuation-Dissipation theorem. Now, looking at Eq. (29) we notice that ξ_i and dt

always appear in the combination $\xi_i dt$. In particular in the random term this may be very annoying because it forces us to use small time steps in order to prevent large velocity changes, which lead to large displacements and finally to wildly fluctuating conservative forces. These problems may be circumvented by eliminating velocities altogether from the description. This we will do in the next subsection. Of course, if we are interested in flow, we will have to come up with a method to measure flow velocities. This we will do in the third subsection of this section.

4.1 Brownian propagator

This section is essentially a simplified version of a paper by Ermak and McCammon[6]. Suppose we are treating a system with very large friction. Characteristic for such systems is that, time intervals Δt exist such that, independent of the velocity at the beginning of the interval, the particle mostly samples velocities from a Maxwell distribution, while at the same time it hardly displaces. By the latter we mean that displacements during time Δt are such that the potential hardly changes. We may therefore choose time intervals Δt such that

$$\frac{1}{\Delta t}\int_t^{t+\Delta t} dt' m_i \frac{d\mathbf{v}_i}{dt'} = \frac{1}{\Delta t}[m_i \mathbf{v}_i(t+\Delta t) - m_i \mathbf{v}_1(t)] \tag{32}$$

is arbitrarily small, while at the same time

$$\frac{1}{\Delta t}\int_t^{t+\Delta t} dt' \nabla_i A(r^{3N}(t')) \approx \nabla_i A(r^{3N}(t)). \tag{33}$$

Let us have a closer look at the meaning of the approximation in the last equation.

Taylor-expanding $\nabla A(r^{3N}(t'))$ we find that the first term that is neglected in Eq. (33) is

$$\sum_j \nabla_i \nabla_j A(r^{3N}(t)) \cdot \frac{1}{\Delta t}\int_t^{t+\Delta t} dt' (\mathbf{r}_j(t') - \mathbf{r}_j(t)). \tag{34}$$

Since we are considering the overdamped case, the dominant contribution to $|\mathbf{r}_j(t') - \mathbf{r}_j(t)|$ is proportional to $(t'-t)^{1/2}$, all other contributions being proportional to $(t'-t)^n$ with $n \geq 1$. After integration over t' and division by Δt this is proportional to $\sqrt{\Delta t}$. All other contributions are proportional to larger powers of Δt. Our approximation therefore implies that we neglect all terms proportional to any power of Δt larger than zero.

Summarizing our results so far, we have

$$0 = -\nabla_i A - \frac{1}{\Delta t}\int_t^{t+\Delta t} dt' \xi_i(t') \mathbf{v}_i(t') + \frac{1}{\Delta t}\int_t^{t+\Delta t} dt' \mathbf{F}_i^{ran}(t') \tag{35}$$

Treating the last two terms similarly to the gradient term, we must evaluate them up to zeroth order in Δt. We start with

$$\frac{1}{\Delta t}\int_t^{t+\Delta t} dt' \xi_i(t') \mathbf{v}_i(t') = \frac{1}{\Delta t}\int_t^{t+\Delta t} dt' [\xi_i(t) + \sum_{j=1}^{N} \nabla_j \xi_i(t) \cdot (\mathbf{r}_j(t') - \mathbf{r}_j(t))] \mathbf{v}_i(t') \tag{36}$$

Performing the integration in the first term and rewriting the second, we obtain

$$\frac{\Delta \mathbf{r}_i(t)}{\Delta t}\xi_i(t) + \sum_{j=1}^{N} \nabla_j \xi_i(t) \cdot \frac{1}{\Delta t}\int_t^{t+\Delta t} dt'(\mathbf{r}_j(t') - \mathbf{r}_j(t))\mathbf{v}_i(t'), \tag{37}$$

where $\Delta \mathbf{r}_i(t) = \mathbf{r}_i(t+\Delta t) - \mathbf{r}_i(t)$. Contributions from potential forces to the integral are at least proportional to $(\Delta t)^2$, so we can restrict attention to contributions from random terms. These are uncorrelated among different particles, so only terms with $i = j$ will contribute. We rewrite the argument of the remaining integral to get

$$\frac{\Delta \mathbf{r}_i(t)}{\Delta t}\xi_i(t) + \nabla_i \xi_i(t) \cdot \frac{1}{2\Delta t}\int_t^{t+\Delta t} dt' \frac{d}{dt'}[(\mathbf{r}_i(t') - \mathbf{r}_i(t))(\mathbf{r}_i(t') - \mathbf{r}_i(t))], \tag{38}$$

where only random displacements should be taken into account. Performing the integral and averaging over all possible realizations, we get

$$\nabla_i \xi_i(t) \cdot \frac{1}{2\Delta t} < (\mathbf{r}_i(t+\Delta t) - \mathbf{r}_i(t))(\mathbf{r}_i(t+\Delta t) - \mathbf{r}_i(t)) >= \frac{k_B T}{\xi_i}\nabla_i \xi_i(t), \tag{39}$$

where we have used Eq. (16).

Collecting terms so far we have

$$0 = -\nabla_i A - \frac{\Delta \mathbf{r}_i}{\Delta t}\xi_i - \frac{k_B T}{\xi_i}\nabla_i \xi_i + \frac{1}{\Delta t}\int_t^{t+\Delta t} dt' \mathbf{F}_i^{ran}(t') \tag{40}$$

Now, consider the last term. Assuming that the friction ξ_i may be taken constant during the time interval Δt, the integral of the random forces may be written as

$$\frac{1}{\Delta t}\int_t^{t+\Delta t} dt' \mathbf{F}_i^{ran}(t') = \frac{1}{\Delta t}\sqrt{2k_B T \xi_i dt}\sum_{k=1}^{\frac{\Delta t}{dt}} \mathbf{\Theta}_{i,k}. \tag{41}$$

First of all, notice that the three Cartesian directions may be treated independently from each other. Next, the sum of N random numbers with mean zero and variance equal to unity is a random number with mean zero and variance equal to N, so

$$\frac{1}{\Delta t}\sqrt{2k_B T \xi_i dt}\sum_{k=1}^{\frac{\Delta t}{dt}} \mathbf{\Theta}_{i,k} = \frac{1}{\Delta t}\sqrt{2k_B T \xi_i dt}\sqrt{\frac{\Delta t}{dt}}\mathbf{\Theta}_i. \tag{42}$$

Introducing this into Eq. (40) and rearranging the result we get after some simple algebra

$$\Delta \mathbf{r}_i = -\frac{1}{\xi_i}\nabla_i A \Delta t + k_B T \nabla_i \frac{1}{\xi_i}\Delta t + \sqrt{\frac{2k_B T \Delta t}{\xi_i}}\mathbf{\Theta}_i. \tag{43}$$

This concludes our derivation of the Brownian propagator.

From now on we do not need to discriminate Δt from dt anymore, so we will replace Δt by dt again. Clearly, the whole procedure that we have gone through for displacements may be repeated for changes in the structural parameters λ^m. This finally leads to the Brownian propagator

$$d\mathbf{r}_i = -\frac{1}{\xi_i}\nabla_i A dt + k_B T \nabla_i \frac{1}{\xi_i} dt + \sqrt{\frac{2k_B T dt}{\xi_i}}\mathbf{\Theta}_i \tag{44}$$

$$d\lambda_s = -\frac{1}{\alpha_s \tau_s}\frac{\partial A}{\partial \lambda_s} dt + \sqrt{\frac{2k_B T dt}{\alpha_s \tau_s}}\Theta_s \tag{45}$$

where we have written the 'friction coefficient' that goes with λ_s as $\alpha_s\tau_s$. So, τ_s is a characteristic time governing the relaxation of λ_s towards its equilibrium value $\lambda_s^{eq}(r^{3N})$. We have assumed that τ_s does not depend on λ_s.

Notice that, whereas time step and friction always occurred as a product ξdt in the Langevin equation, they appear as a fraction $\frac{dt}{\xi}$ in the Brownian propagator. This means that with increasing frictions increasingly larger time steps can be used.

4.2 Memory

It is instructive[7] to formally integrate Eq. (45) and put the result into the equation that describes the dynamics of positions, Eq. (44). When doing so, we will neglect the random contribution in Eq. (45). Using the expression for Φ^t in Eq. (26) and assuming that all λ_s are equal to zero at time zero, we obtain

$$-\nabla_i\Phi^t = \sum_{s=1}^{m}\alpha_s[\frac{1}{\tau_s}\int_0^t dt'\lambda_s^{eq}(r^{3N}(t'))e^{-(t-t')/\tau_s} - \lambda_s^{eq}(r^{3N}(t))]\nabla_i\lambda_s^{eq}(r^{3N}(t)). \tag{46}$$

There are many ways to rewrite this equation. We restrict ourselves to just one of them. We rewrite the integral in the right hand side according to

$$\frac{1}{\tau_s}\int_0^t dt'\int_0^{t'} dt''\frac{d\lambda_s^{eq}}{dt''}e^{-(t-t')/\tau_s} = \frac{1}{\tau_s}\int_0^t dt''\int_{t''}^t dt'\frac{d\lambda_s^{eq}}{dt''}e^{-(t-t')/\tau_s}. \tag{47}$$

Next we perform the integral ove t' and write $\lambda_s^{eq}(t)$ as an integral of its derivative from time zero to time t, obtaining

$$-\nabla_i\Phi^t = -\sum_{s=1}^{m}\alpha_s\int_0^t dt'\frac{\partial\lambda_s^{eq}}{dt'}e^{-(t-t')/\tau_s}\nabla_i\lambda_s^{eq}(r^{3N}(t)). \tag{48}$$

Performing some cosmetic actions, this may be written in the suggestive form

$$-\nabla_i\Phi^t = -\sum_{j=1}^{N}\int_0^t d\mathbf{r}_j(t')\cdot[\sum_{s=1}^{m}\alpha_s\nabla_j\lambda_s^{eq}(r^{3N}(t'))\nabla_i\lambda_s^{eq}(r^{3N}(t))e^{-(t-t')/\tau_s}], \tag{49}$$

which has a strong resemblance to the generalized friction introduced earlier.

Let us now have a closer look at what type of variables can be used as structure parameters λ_s. We will illustrate our discussion again using the example of star polymers. The left most part of Fig. (2) shows two stars equilibrated at a distance r_{ij}. Next, these two stars are quickly displaced to a new distance r_{ij}^{new}. It is clearly seen that the arms of the stars are 'torn apart' and will need some time to adjust to the new situation. As time passes by, the arms more and more relax, until in the rightmost picture they have found the equilibrium configuration that goes with the new distance r_{ij}^{new}. We therefore define structure parameters λ_{ij} with every pair of particles (i,j) at distances smaller than some cutoff value R_c, not necessarily the same as in section (4.4) below. The corresponding equilibrium values $\lambda_{ij}^{eq}(r_{ij})$ depend on the distance r_{ij} between the two particles.

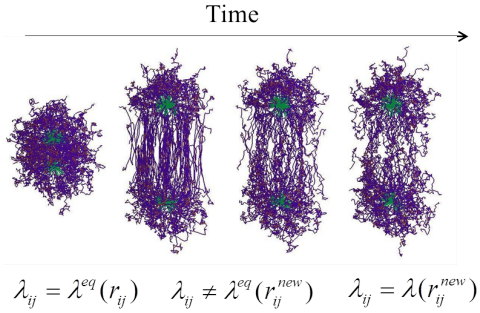

Figure 2: Two stars at equilibrium in the leftmost panel, displaced to a new distance in the second panel and next relaxing towards equilibrium at the new distance, which they reach in the rightmost panel. The thermodynamic state of the arms is described by a structural parameter λ_{ij} which equals $\lambda_{ij}^{eq}(r_{ij})$ in the leftmost panel and $\lambda_{ij}^{eq}(r_{ij}^{new})$ in the rightmost panel.

4.3 Equilibrium

We now ask what is the equilibrium distribution that goes with the Brownian propagator. We present our arguments for the case of a independent particles in a potential A. Generalization to the case of a dense suspension of particles is then obvious.

In general we may say that the probability $G(\mathbf{r})d^3r$ to find the particle in a cube of volume $d^3r = dxdydz$ evolves according to

$$\frac{\partial}{\partial t}G(\mathbf{r}) = -\nabla \cdot \mathbf{J}(\mathbf{r}), \tag{50}$$

where $\mathbf{J}$ is the flux of particles, *i.e.* the number of particles that go through unit area, per unit of time. Equilibrium occurs when the flux is equal to zero. The flux in our case may readily be understood to be given by

$$\mathbf{J}(\mathbf{r}) = -\frac{1}{\xi}G(\mathbf{r})\nabla A(\mathbf{r}) + k_B T G(\mathbf{r})\nabla\frac{1}{\xi(\mathbf{r})} + \mathbf{J}^{ran}(\mathbf{r}), \tag{51}$$

where $\mathbf{J}^{ran}(\mathbf{r})$ is the contribution from the random displacements made by the particles. Since random displacements in the three Cartesian directions are independent, we may restrict ourselves to treating just one of these.

Consider a plane of unit area at position x. The number of particles that pass through this plane during time Δt by making a step of size between Δ and $\Delta + d\Delta$ in positive x-direction is given by

$$\frac{1}{2}G(x-\Delta/2)P_{\Delta t}(x-\Delta/2;\Delta)\Delta d\Delta. \tag{52}$$

Here $P_{\Delta t}(x;\Delta)d\Delta$ is the probability that a particle at position x during time Δt makes a step of size between Δ and $\Delta + d\Delta$in positive x-direction. The factor of one half takes into account that only half of the particles move in positive direction. With a similar expression for particles passing through the plane in negative direction we obtain an overall contribution to J_x^{ran} from particles through the plane with step-size between Δ and $\Delta+d\Delta$

$$\frac{1}{2}G(x-\Delta/2)P_{\Delta t}(x-\Delta/2;\Delta)\Delta d\Delta - \frac{1}{2}G(x+\Delta/2)P_{\Delta t}(x+\Delta/2;\Delta)\Delta d\Delta. \tag{53}$$

After Taylor expanding G and $P_{\Delta t}$ to first order in Δ we obtain

$$-\frac{1}{2}\frac{\partial G(x)}{\partial x}P_{\Delta t}(x;\Delta)(\Delta)^2 d\Delta - \frac{1}{2}G(x)\frac{\partial}{\partial x}P_{\Delta t}(x;\Delta)(\Delta)^2 d\Delta. \tag{54}$$

We next integrate over all values of Δ and divide by Δt, obtaining

$$J_x^{ran} = -\frac{\partial G(x)}{\partial x}\frac{k_B T(x)}{\xi(x)} - G(x)\frac{\partial}{\partial x}\frac{k_B T(x)}{\xi}. \tag{55}$$

Generalizing to three Cartesian coordinates we obtain for the total flux

$$\mathbf{J}(\mathbf{r}) = -\frac{1}{\xi\mathbf{r})}G(\mathbf{r})\nabla A(\mathbf{r}) + k_B T(\mathbf{r})G(\mathbf{r})\nabla\frac{1}{\xi(\mathbf{r})} - \nabla[G(\mathbf{r})\frac{k_B T(\mathbf{r})}{\xi(\mathbf{r})}]. \tag{56}$$

We have included the possibility that the temperature depends on the position of the particle.

Now let us draw a few conclusions. First, rewrite the flux as

$$\mathbf{J}(\mathbf{r}) = -\frac{1}{\xi(\mathbf{r})}G(\mathbf{r})\nabla A(\mathbf{r}) - \frac{k_B T(\mathbf{r})}{\xi(\mathbf{r})}\nabla G(\mathbf{r}) - \frac{1}{\xi(\mathbf{r})}G(\mathbf{r})\nabla k_B T(\mathbf{r}). \tag{57}$$

We find that besides external forces, both concentration gradients and temperature gradients give rise to fluxes. Fluxes due to temperature gradients are called Soret fluxes.

Next, assume that the temperature is constant throughout the system. Putting the flux equal to zero, we find that the distribution is proportional to the Boltzmann factor, *i.e.*

$$G(\mathbf{r}) \propto e^{-A(\mathbf{r})/k_B T}. \tag{58}$$

So, the statistical equilibrium distribution gives rise to zero flux, as expected.

Finally, it is not difficult to understand that the equilibrium distribution that goes with Eqs (44,45) is given by

$$G(r^{3N}, \lambda^m) \propto e^{-A(r^{3N},\lambda^m)/k_B T}. \tag{59}$$

Integrating the last equation over all possible values of the λ_s we obtain

$$\begin{aligned} G(r^{3N}) &\propto \int d\lambda^m e^{-A(r^{3N},\lambda^m)/k_B T} \\ &= e^{-\Phi(r^{3N})/k_B T}\int d\lambda^m e^{-\frac{1}{2}\sum_{s=1}^{m}\alpha_s(\lambda_s-\lambda_s^{eq}(r^{3N}))^2/k_B T} \\ &\propto e^{-\Phi(r^{3N})/k_B T}. \end{aligned} \tag{60}$$

The distribution of configurations r^{3N} in the stationary state is therefore equal to the exact equilibrium distribution of the system (provided $\Phi(r^{3N})$ faithfully represents the free energy of the structural parameters as defined in Eq.(20)). As a result thermodynamic properties simulated with this model will be the exact thermodynamic properties of the system.

4.4 Flow

As they stand, our equations of motion, Eqs (44) and (45), are not Galilei invariant. In order to achieve this, we include an affine displacement $\mathbf{V}(\mathbf{r}_i)dt$ in the right hand side of Eq. (44). Notice that this term would have appeared automatically had we started our derivation of the Brownian propagator with a Langevin equation including a local velocity term. So its physical meaning is the same as in the Langevin equation. It is a background flow field with respect to which the particles move and experience friction forces.

Now this forces us to invent a way to calculate the local velocity $\mathbf{V}(\mathbf{r}_i)$ at the position of particle i. One way is to make use of a predefined velocity field obtained on the basis of some macroscopic phenomenological theory. If we want the flow to develop itself as a result of applied forces and boundary conditions, however, this will not do. We will assume that the background flow at position $\mathbf{r}$ may be obtained as some local average of the drift velocities of the particles near $\mathbf{r}$, drift velocities being defined as displacements defined by time intervals. Moreover, we assume that a good representation of the background flow field may be obtained by giving its value at a discrete set of points, for which we choose the positions of the particles. Defining $\mathbf{v}_i = \mathbf{V}(\mathbf{r}_i)$ it is possible to motivate the following update scheme for the local velocities $\mathbf{v}_i$

$$d\mathbf{v}_i = \frac{1}{\tau_f}[-\frac{1}{\xi_i}\nabla_i A + \sum_{j=1}^{N} f_{ij}(r_{ij})(\mathbf{v}_j - \mathbf{v}_i)]dt + \sum_{j=1}^{N}\sqrt{\frac{2k_BT}{\xi_i}f_{ij}}\frac{\mathbf{\Theta}_{ij}}{\tau_f}, \qquad (61)$$

where the random pair vectors must be such that $\mathbf{\Theta}_{ij} = -\mathbf{\Theta}_{ji}$. The functions f_{ij} are defined according to

$$f_{ij}(r_{ij}) = \frac{15}{2\pi R_c^3}\xi_j(\frac{1}{\rho_i} + \frac{1}{\rho_j})(1 - \frac{r_{ij}}{R_c})^3$$

$$\rho_i = \frac{21}{2\pi R_c^3}\sum_{j=1}^{N}\xi_j(1 - \frac{r_{ij}}{R_c})^4(4\frac{r_{ij}}{R_c} + 1). \qquad (62)$$

Here R_c is some cutoff distance such that on average about 15 particles contribute to the sum in ρ. We refer for further details to Padding and Briels[8].

When dealing with flowing matter, choosing the correct propagator is only part of the story. In case one is interested in the influence of hydrodynamics on equilibrium properties one can perform simulations with periodic boundary conditions. This has been done in the paper by Padding and Briels[8] and it was found that all theoretical results are reproduced correctly. If one is interested in flow instabilities that occur in the bulk of the system, non-equilibrium simulations with Lees-Edwards boundary conditions may be performed. This has been done to study shear banding with a variety of systems. The example of telechelic polymers will be discussed below. If, however, interest lies in systems with hard walls, one has to come up with the correct way to implement stick our partially stick boundary conditions. These methods have been developed for standard simulations, but for the present model are still under construction.

5 Telechelic Polymers

I will restrict myself to discussing one example of a simulation performed with the RaPiD scheme.

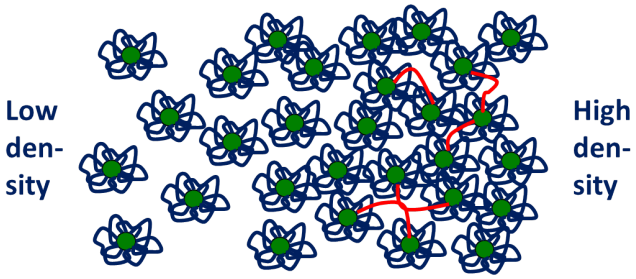

Figure 3: 3-block copolymers dissolved in water with increasing concentration from left to right. The two outer blocks are hyprophobic (green) and the middle block hydrophylic (blue). The hydrophobic middle blocks of some twenty polymers gather together to form micelles, while the middle blocks are dissolved in the solvent. At low concentrations micelles exist as independent flowers. At higher concentrations the two outer blocks of one polymer do not necessarily take part in one and the same micelle, but may be part of two different micelles, thereby forming bridges between them. Bridges are colored red for visualization purposes only.

In Fig. (3) a solution of 3-block co-polymers is depicted. In the left hand side of the figure the concentration is low, while in the right hand side it is large. The two outer blocks of the polymer are hydrophobic (green) while the inner block is hydrophylic (blue). At low concentrations the stars look like flowers. The outer, hydrophobic blocks of some twenty polymers have gathered together to form a micelle, thereby minimizing the unfavorable interaction with the solvent. The middle blocks are dissolved in the solvent. With increasing concentrations the hydrophonic outer blocks may take part in two different micelles, thereby establishing a bridge between the two micelles. These bridges severely influence the rheological properties of the fluid.

As mentioned above, the transient potential is assumed to be a pairwise sum of all pairs within a predescribed cutoff distance

$$\Phi^t(r^{3N}, \lambda^m) = \frac{1}{2} \sum_{i=1}^{N-1} \sum_{j=i+1}^{N} \alpha(\lambda_{ij} - \lambda_{ij}^{eq}(r_{ij}))^2. \tag{63}$$

The meaning of the λ_{ij} ia taken to be the number of bridges between particles i and j. Then it is reasonable to assume that all α's are equal. Moreover the thermodynamic potential in this case is best represented by a sum of pair potentials as well. The pair contributions were calculated by means od Scheutjens-Fleer theory. All parameters in the model were known except α. For more information see Sprakel *et. al.*[9]. In Fig. (4) we present the results of our calculations of viscosities together with experimental values. The experimental viscosities were used to fit the only unknown parameter in the model. The interesting point is that viscosities vary by five orders of magnitude when the concentratios vary by three orders of magnitude, yet all of this can be reproduced by adjusting only one parameter.

Encouraged by our result so far, we now try to go for predictions. To this end we have performed non-equilibrium simulations in which the systems are sheared according to well established methods in simulation country. In Fig. (5) results are shown for a system with concentration of 20 gram/liter and a shear rate of $4/\tau$, where τ is the characteristic time occurring in the propagator for λ_{ij}. In the left panel, upper figure the stress is plotted as function of time lapse since the start of the run. It is clearly seen that, initially, the stress is constant, but, after some time, begins to drop until it reaches a new stationary value. In

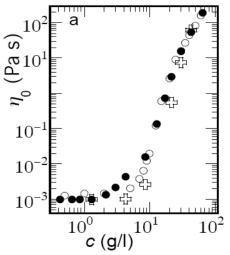

Figure 4: Viscosities versus concentration. Open circles are experimental values and crosses are theoretical results. The black circles are the results of simulations with artificially enlarged frictions. The reason for doing so is that these larger frictions allow larger time steps and therefore shorter simulations. As can be seen changing the friction to (incorrect) larger values only influences the results at small concentrations. This tells us that, while at low concentrations viscosities are determined by frictions with the solvent, at higher concentrations viscosities are determined by interactions between the particles, as expected.

the left panel, lower figure the flow velocity in x-direction is plotted for various equidistant positions along the gradient direction. In a normal situation, with a constant shear rate at all positions along the gradient direction, all lines would be parallel and equidistant (since the velocity would linearly increase along the gradient direction). We see however, that concomitantly with the drop of the stress velocities begin to change until after some time the velocities in a number of planes along the gradient direction differ from each other by only very small amounts. One may say that the system has split into two parts, one in which the shear rate is large, and one in which the shear rate is very low. In the example discussed here, the band with the lower shear rate has a somewhat larger concentration than the one with the higher shear rate. As a result the two bands can easily be visualized as seen in the right panel. The phenomenon just described is called shear banding, and has been theoretically analyzed by Dhont[10]. It is important to notice that banding would not have occurred in our simulations had we imposed a linear flow field instead of measured the background flow as described in the theory section.

In Fig. (6) we show some quantitative results for the banding observed with the system of Fig. (5). In the left panel we present the concentrations in the two bands as a function of applied shear rate. In cases when no banding occurs, the concentration is constant and equal to 20 gram/liter. For shear rates when banding does occur, two concentrations are given, one for each band. As can be seen they clearly differ. In the right panel, shear rates in the two bands are plotted as a function of the applied shear rate. Again, when no banding occurs, the system is homogeneously sheared with only one shear rate, equal to the applied shear rate. In this case, also experimental results are available (open circles), and it is seen that experiment and simulations are very well in agreement.

6 Concluding Remarks

In this paper we have reviewed the standard examples of stochastic dynamics simulations and adjusted them to be applicable to simulate the flow of complex soft matter in complex geometries. The changes needed to accommodate to soft matter systems consisted

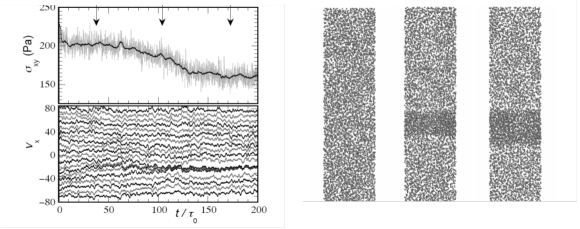

Figure 5: Results from non-equilibrium simulations with telechelic systems of concentrations equal to 20 gram/liter and shear rates equal to $4/\tau$. Left upper figure shows tresses as function of time lapse since the start of the run. After some initial period of constant stresses, the stresses begin to drop to lower values until they reach a new stationary value. Concomitantly with the stress drop the velocity field changes (left lower figure) such that the system splits into two bands, one of which has a shear rate smaller than the applied shear rate, while the other has a shear rate larger that the applied shear rate. Since the concentrations in the two bands differ, the bands can be easily observed, as shown in the right part of the figure. In these figures, flow is from left to right with increasing velocities from bottom to top. The ratio between flow velocity and vertical position is the shear rate. In the dark bands shear rates are less then in the lighter bands.

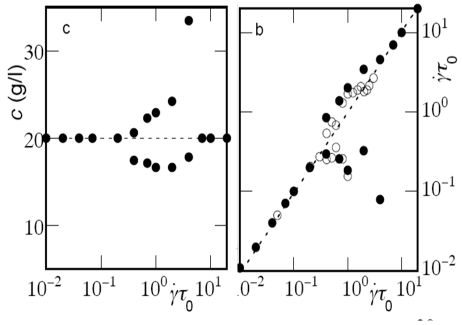

Figure 6: Quantitative results from the simulations described in Fig. (5). In the left panel the concentrations in the two bands are plotted as a function of the applied shear rates. When no banding occurs the concentration is constant throughout the box and equal to the overall concentration. When banding occurs the concentration in the high shear rate band is less than the overall concentration while that in the low shear rate band is larger than the overall concentration. In the right panel the corresponding shear rates are plotted as a function of the imposed shear rates. In this case experimental results are available and seen to be in very good agreement with the simulated results.

of inclusion of memory, adjusting the method to overdamped systems and guaranteeing hydrodynamics also for the Brownian propagator.

I have presented results for only one system, solutions of telechelic polymers. Several more systems have been successfully simulated by now. The linear rheology of linear polymers was shown to be well represented by the RaPiD model for frequencies just beyond the first crossing point of the shear and loss moduli. Non linear rheology was well reproduced up to rather high shear rates. One of the success stories of the method has been with pressure sensitive materials where both shear and elongational viscosities were well reproduced. In times where The Web of Science plays an important role in rating scientists